Acta Pharmaceutica Sinica B 2023;13(7):3027−3042

Chinese Pharmaceutical Association
Institute of Materia Medica, Chinese Academy of Medical Sciences

Acta Pharmaceutica Sinica B

www.elsevier.com/locate/apsb
www.sciencedirect.com

ORIGINAL ARTICLE

A novel mesenchymal stem cell-based regimen for acute myeloid leukemia differentiation therapy

Luchen Sun[a,†], Nanfei Yang[b,†], Bing Chen[e], Yuncheng Bei[d], Zisheng Kang[f], Can Zhang[f], Nan Zhang[g], Peipei Xu[e], Wei Yang[h], Jia Wei[d], Jiangqiong Ke[a], Weijian Sun[a,*], Xiaokun Li[i,*], Pingping Shen[a,c,j,*]

[a]*The Second Affiliated Hospital and Yuying Children's Hospital of Wenzhou Medical University, Wenzhou 325027, China*
[b]*School of Pharmaceutical Science, Wenzhou Medical University, Wenzhou 325035, China*
[c]*Department of Urology, Drum Tower Hospital, Medical School of Nanjing University, Institute of Urology, Nanjing University, Nanjing 210008, China*
[d]*The Comprehensive Cancer Centre of Nanjing Drum Tower Hospital, the Affiliated Hospital of Nanjing University Medical School, Nanjing University, Nanjing 210008, China*
[e]*Department of Hematology, the Affiliated Drum Tower Hospital of Nanjing University Medical School, Nanjing 210093, China*
[f]*State Key Laboratory of Natural Medicines and Jiangsu Key Laboratory of Drug Discovery for Metabolic Diseases, Center of Drug Discovery, China Pharmaceutical University, Nanjing 210009, China*
[g]*Centre of Micro/Nano Manufacturing Technology (MNMT-Dublin), School of Mechanical & Materials Engineering, University College Dublin, Dublin 4, Ireland*
[h]*Department of Surgery, Division of Cancer Biology and Therapeutics, Cedars-Sinai Medical Center, Los Angeles, CA 90048, USA*
[i]*Oujiang Laboratory (Zhejiang Lab for Regenerative Medicine, Vision and Brain Health) & School of Pharmaceutical Science, Wenzhou Medical University, Wenzhou 325035, China*
[j]*Shenzhen Research Institute of Nanjing University, Shenzhen 518000, China*

Received 16 October 2022; received in revised form 5 March 2023; accepted 14 March 2023

*Corresponding authors.
E-mail addresses: xiaokunli@wmu.edu.cn (Xiaokun Li), ppshen@nju.edu.cn (Pingping Shen), fame198288@126.com (Weijian Sun).
[†]These authors made equal contributions to this work.
Peer review under the responsibility of Chinese Pharmaceutical Association and Institute of Materia Medica, Chinese Academy of Medical Sciences.

https://doi.org/10.1016/j.apsb.2023.05.007

KEY WORDS

Mesenchymal stem cell;
Acute myeloid leukemia;
Extracellular vesicles;
Nonsteroidal VDR modulators;
Combination therapy

Abstract Currently the main treatment of acute myeloid leukemia (AML) is chemotherapy combining hematopoietic stem cell transplantation. However, the unbearable side effect of chemotherapy and the high risk of life-threatening infections and disease relapse following hematopoietic stem cell transplantation restrict its application in clinical practice. Thus, there is an urgent need to develop alternative therapeutic tactics with significant efficacy and attenuated adverse effects. Here, we revealed that umbilical cord-derived mesenchymal stem cells (UC-MSC) efficiently induced AML cell differentiation by shuttling the neutrophil elastase (NE)-packaged extracellular vesicles (EVs) into AML cells. Interestingly, the generation and release of NE-packaged EVs could be dramatically increased by vitamin D receptor (VDR) activation in UC-MSC. Chemical activation of VDR by using its agonist 1α,25-dihydroxyvitamin D3 efficiently enhanced the pro-differentiation capacity of UC-MSC and then alleviated malignant burden in AML mouse model. Based on these discoveries, to evade the risk of hypercalcemia, we synthetized and identified sw-22, a novel non-steroidal VDR agonist, which exerted a synergistic pro-differentiation function with UC-MSC on mitigating the progress of AML. Collectively, our findings provided a non-gene editing MSC-based therapeutic regimen to overcome the differentiation blockade in AML.

1. Introduction

Acute myeloid leukemia (AML) is a heterogeneous clonal disorder characterized by the accumulation of malignant, immature myeloid blasts. The leukemic blasts are arrested at an early stage of differentiation and become tumorigenic clones with a growth advantage[1]. All-*trans*-retinoic acid and arsenic trioxide therapy dramatically improves the prognosis of acute promyelocytic leukemia, and represents the only clinical advance in pro-differentiation therapy in AML[2,3]. This indicates that differentiation therapy, which has the goal of inducing malignant cells to overcome the differentiation blockade, provides an alternative clinical avenue for AML. Moreover, hematopoietic stem cell transplantation (HSCT) combined with high-dosage chemotherapy is currently considered the standard of care for patients with poor-risk AML[4]. However, the high incidence of post-transplantation disease relapse limits the application of HSCT for AML[5,6]. These dissatisfactory outcomes highlight the need for efficacious and alternative therapeutic approaches to treat AML.

Adoptive transfer of mesenchymal stem cells (MSC) has been successfully employed to treat certain vicious diseases. Notably, as reported on clinicaltrials.gov, there have been clinical trials investigating the efficiency of MSC in hematologic malignancy. For instance, human adipose-derived MSC inhibited chronic myeloid leukemia cell proliferation by secreting Dickkopf-related protein 1[7]. Mouse bone marrow-derived MSC suppressed lymphoma and leukemia cell proliferation *in vitro*[8]. Emerging data have reported that MSC suppressed proliferation and induced apoptosis of blood malignant cells[9], while the efficacy of MSC treatment in the fate determination of AML cells remains unclear. Moreover, uncovering the underlying mechanisms and identifying the related key node controller in regulating the anti-AML activity of MSC are beneficial for designing novel MSC-based therapeutic regimens to treat AML.

In this study, we demonstrated that human umbilical cord derived MSC (UC-MSC, mentioned as MSC below) exerted their marked pro-differentiation effects on primary AML patient cells and reduced leukemia burden in an AML mouse model. Mechanistically, extracellular vesicles (EVs) secreted by MSC played a predominate role in initiating AML cell differentiation *via* transporting neutrophil elastase (NE) into AML cells. Importantly, we identified vitamin D receptor (VDR) as the key node to regulate the generation and release of NE-packed EVs from MSC. Chemical activation of VDR by using its agonist dramatically increased NE-packed EVs release from MSC and enhanced MSC-mediated anti-AML effects *in vivo* and *in vitro*. Thus, sw-22, a novel structural nonsteroidal VDR agonist without causing hypercalcemia, was designed and synthesized successfully. This small molecule exhibited an intriguing synergistic effect with MSC on inducing AML cell differentiation *via* enhancing the generation of NE-packed EVs. Finally, modulating VDR activity in MSC through treatment with chemical agonist suppressed AML progression *in vivo*, thus supporting potential clinical applications for inducing AML cell differentiation.

2. Materials and methods

2.1. Cell line and cell culture

Primary leukemia cells and UC-MSC were obtained from Nanjing Drum Tower Hospital (Nanjing, China) after informed consent. UC-MSC were cultured in alpha-MEM medium. Primary leukemia cells, U937 cells and THP-1 cells were cultured in RPMI 1640. All media were supplemented with 10% fetal bovine serum and maintained in a humidified incubator at 37 °C with 5% CO_2.

2.2. In vitro differentiation assay

For Transwell co-culturing AML cells with MSC, MSC (1×10^5) were seeded and acclimated in the 12-well plates overnight. Then, the Transwell inserts were placed in the plates, and AML cells (3×10^5) were added in the top. For cell−cell contact co-culture, MSC (1×10^5) were seeded into 12-well plates and acclimated overnight. AML cells (3×10^5) in complete medium were added to the MSC culture with or without 1α,25-dihydroxyvitamin D3 (1,25D3) (MCE), Y27632 (MCE), SB239063 (MCE) or Stattic (Sigma−Aldrich). After 48 h, the AML cells were collected, and their differentiation was determined by fluorescence-activated cell sorting (FACS).

2.3. Flow cytometry

Single-cell suspensions of leukemic cells from BM and blood of treated mice, and AML cell lines were stained for 30 min on ice with various antibodies: CD11b-PE (ICRF44; eBioscience), CD14-FITC (M5E2; Biolegend), CD14-PerCpCy5.5 (M5E2; BD), CD45-FITC (HI30; BD/2D1; eBioscience). The apoptotic cells were measured by AnnexinV/PI according to manufacturer's protocol (BD Biosciences). Phagocytosis assays were conducted by using fluorescent red latex beads (1 μmol/L diameter, L-2778, Sigma−Aldrich). The cells were analyzed on a FACSCalibur cytometer using CellQuest software (BD Biosciences). The data were analyzed using FlowJo software. The statistics presented are derived from at least 10,000 events from the gated population of interest.

2.4. TMT-based mass spectrometric analysis

MS analysis on the secretome of MSC was performed as previously reported[10]. Briefly, approximately 1×10^6 MSC were seeded in a T75 flask overnight, then MSC were incubated with 3×10^6 U937 cell for 48 h. Then, U937 cells were removed, and MSC were washed three times in PBS. MSC were cultured with 10 mL serum-free medium for 24 h. Next, serum-free conditional medium (CM) was harvested and centrifuged at 10,000 × *g* to remove the cell debris. The CM was concentrated with ultrafiltration conical tubes with membranes selective for molecules <10 kDa (Millipore UFC501096) five times at 4000 × *g* for 30 min each time. Finally, the concentrated samples were analyzed with MS/MS.

2.5. Bioinformatic analysis

Gene Ontology (GO) enrichment analyses were performed by using the ClusterProfiler (v3.16.0) R package. Weighted gene co-expression network analysis (WGCNA) was conducted using the WGCNA (1.69) package. The module eigengene expression, adjacency matrix heatmap, module-trait relationships, and other related parameters were calculated and visualized according to package instructions.

2.6. RNA isolation and quantitative real time PCR

Total RNA was isolated from MSC or AML cells with TRIzol reagent (Invitrogen), and the protocol was followed according to the manufacturer's instructions, and then RNA was quantified with Nano-drop. Reverse transcription was performed with 5 × All-In-One RT MasterMix (abm Cat#G486 Code Q111-02) kit. Quantitative-PCR assays were carried out on the CFX96 real time PCR detection system (Bio-Rad). The comparative threshold method for relative quantification was used, and the results are expressed as fold change. The expression of the measured genes in each sample was normalized to the *GAPDH* mRNA expression levels. The details of primers are listed in Supporting Information Table S1.

2.7. Western blotting

After treatment, the cells were harvested, and the proteins were extracted by whole cell lysis (Beyotime). Protein concentration was determined by BCA reagent from Pierce. Lysates were eluted in 1 × SDS Loading Buffer (Beyotime), resolved by 10% SDS-polyacrylamide gels, transferred to PVDF membranes (Bio-Rad) and then probed with the appropriate antibodies. The LumiGlo Chemiluminescent Substrate System (Thermo) was used for protein detection. The antibodies used were specific for Cyclin D1 (bs-0572R, Bioss), p21 (sc-6246; Santa Cruz), Alix (18269, CST), Flotillin-1 (18634, CST), Annexin V (8555, CST), Neutrophil Elastase (63610,CST), Neutrophil Elastase (bs-6982R, Bioss), p38 MAPK (9212, CST), p-p38 MAPK (T180/Y182) (9215, CST), p-STAT3 (Y705) (9145, CST), STAT3 (9132; CST), VDR (14526-1-AP; Proteintech), GAPDH (1:10,000; MB001H, Bioworld) and β-actin (1:10,000; ab133626, Abcam). All antibodies were used at a 1:1000 dilution for Western blotting unless otherwise noted.

2.8. EVs experiments

EVs from MSC culture medium were isolated as previously described[11]. In brief, MSC were cultured with EV-depleted FBS for 48 h. Then, culture medium was collected and centrifuged at 3000 × *g* for 10 min at 4 °C, followed by a centrifugation step of 10,000 × *g* for 30 min at 4 °C to remove cellular debris. EVs were isolated using ultracentrifuge at 100,000 × *g* for 90 min. The pellet was washed with ice-cold PBS, resuspended in PBS and stored at −80 °C. EVs quantification was performed by determination of the protein contents using a bicinchoninic acid assay. The amount of EVs was also quantified by using BCA method. EVs were examined by transmission electron microscope (TEM). Primary antibodies against Alix, Flotillin-1 and Annexin V were used for the identification of EVs. For the visualization of EV-packaged NE internalization, MSC were transfected by lentiviral particles expressing GFP-labelled NE. After 48 h, the culture medium of transfected MSC was collected and isolated for EVs. The collected EVs were added to AML cells. Images were obtained by laser scanning confocal microscopy.

For *in vitro* experiments, 10 μg/mL MSC-EVs or PBS control were added into the U937 or THP-1 cells culture medium, and then incubated for 48 h to ensure incorporation of the MSC-EVs. For *in vivo* studies, NOD/SCID mice which were intravenously injected with AML cells three days followed by injected with 100 μg MSC-EVs (diluted in 200 μL saline) or 1×10^6 MSC per mouse *via* tail vein. AML mice that received the equivalent volume of saline were considered as the control group.

2.9. Lentiviral plasmids production and cell infection

The cDNAs encoding GFP-labelled NE or VDR were cloned, and inserted into the pLenti6/v5 lentiviral vector. The lentiviral particles were produced in HEK293T cells by co-transfecting the plasmids with two package plasmids (psPAX2 and pMD2.G) using Lipofectamine 2000 (Invitrogen). Culture supernatants were collected after transfection for 72 h. The medium containing concentrated lentivirus (Lenti-Concentin Virus Precipitation Solution, Cat. No. C103-01) was used to infect MSC.

2.10. Animal studies

The xenograft leukemia model was established by the direct intravenous injection of U937 cells (1×10^7) into the tail veins of NOD/SCID mice purchased from the Model Animal Research Center of Nanjing University (Nanjing, China). Three days after implantation, the mice were grouped and intravenously injected *via* the tail vein with MSC (1×10^6) per week combined with sw-

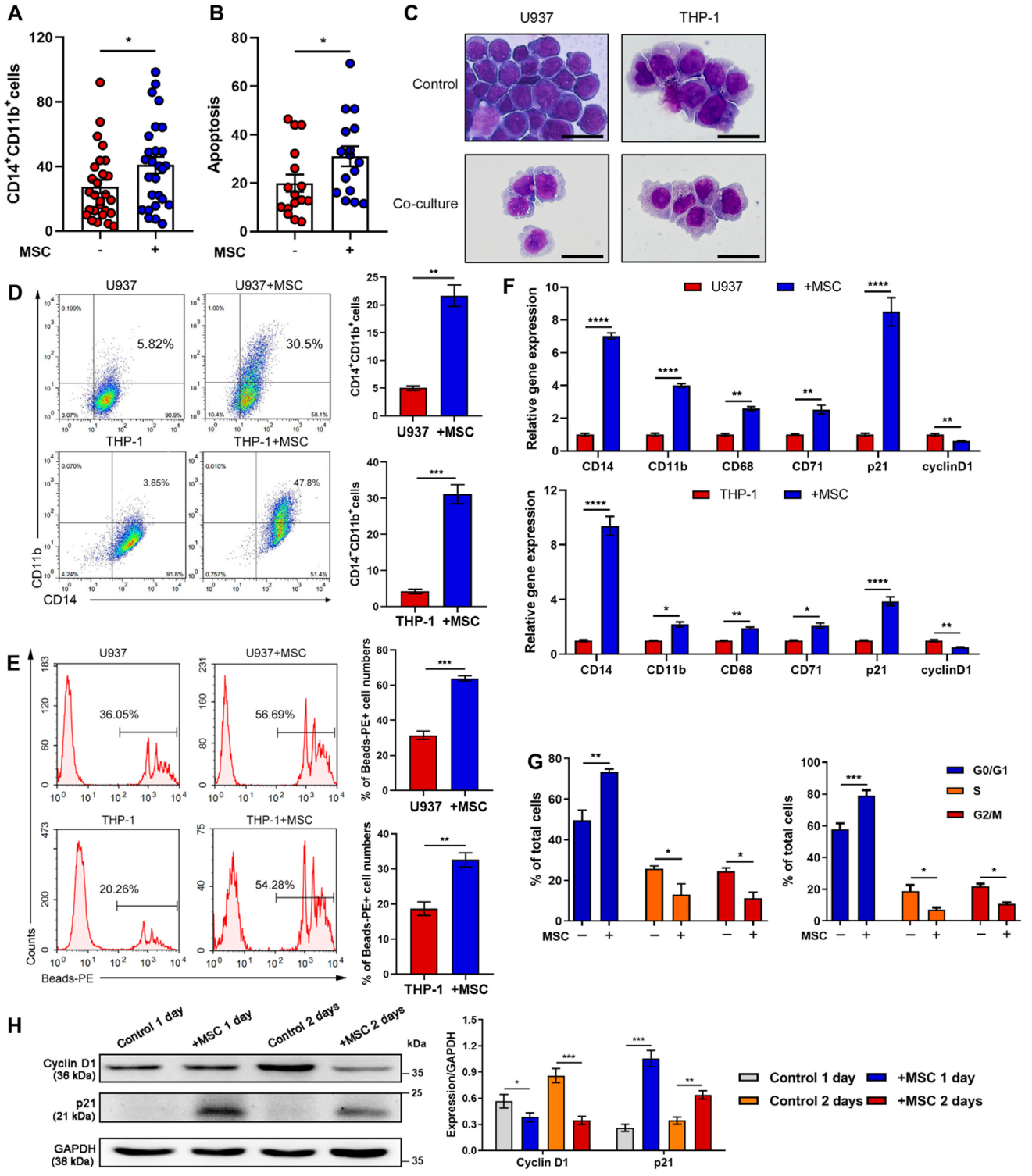

Figure 1 MSC treatment induces AML cell differentiation. (A, B) Flow cytometry for $CD14^{+}CD11b^{+}$ (A) and apoptotic (B) primary human cells from M4 and M5 patients after MSC incubation. Each dot represents one patient. (C) U937 and THP-1 cells were co-cultured with MSC for 48 h, morphological changes accompanied by myeloid differentiation were confirmed by Wright−Giemsa staining of cells. Scale bar = 25 μm. (D, E) Flow cytometry analysis of the expressions of the differentiation markers CD11b and CD14 (D) and the phagocytosis activity (E) ($n = 3$). (F) The relative gene expression levels of the differentiation and cell cycle markers *CD14*, *CD11b*, *CD68*, *CD71*, *p21* and Cyclin D1 in U937 and THP-1 cells were assessed by RT-qPCR ($n = 3$). (G) Flow cytometry analysis of the cell cycle arrest of U937 and THP-1 cells co-cultured with MSC for 48 h ($n = 3$). (H) Protein levels of Cyclin D1 and p21 were both upregulated in cocultured U937 cells; the results were detected by Western blotting. Data are quantified on the right. Data are represented as the mean ± SEM. Data were analyzed by Student's *t* test (D, E), two-way ANOVA followed by Bonferroni's test (F, G). $^{*}P < 0.05$, $^{**}P < 0.01$, $^{***}P < 0.001$, $^{****}P < 0.0001$.

22 (10 mg/kg) or 1,25D_3 (0.3 μg/kg) or with phosphate buffered-saline intraperitoneally 5 times per week for 4 weeks. All mouse procedures and experiments for this study were approved by the Institutional Animal Care and Use Committee at Nanjing University (No. ICAUC-2007021).

2.11. H&E staining and immunofluorescence

Formalin-fixed, paraffin-embedded samples were segmented and stained with hematoxylin and eosin (H&E). The cell slides were fixed and stained with anti-CD45 (sc-1178, Santa Cruz) antibodies. Images were acquired using a Nikon A1R confocal laser scanning microscope. The TIFF files were imported into Adobe Photoshop, and the entire field was enhanced and sharpened using the levels command and/or a high-pass filter.

2.12. Statistical analysis

Statistical analysis was performed using GraphPad Prism 6.0 software. Error bars indicate the standard error of the mean (SEM) unless otherwise indicated. The differences were analyzed by using a nonparametric Mann−Whitney analysis (two-tailed). *P* values of the plotted data ≤ 0.05 were considered statistically significant. All statistical analyses were generated based on at least three independent experiments.

3. Results

3.1. MSC treatment confers AML cells monocyte-like phenotype

In the preliminary clinical study, we designed an experiment utilizing MSC to treat acute leukemia cells to evaluate the impact of MSC on leukemia cells. We collected peripheral blood samples from 27 AML patients and conducted an analysis to monitor the phenotypic characteristics of the AML cells after a 48 h incubation with MSC. The data revealed that the expression levels of both CD11b and CD14, two typical surface markers of monocyte differentiation, increased in 22 of 27 primary AML cells, indicating that AML cells might undergo differentiation mediated by MSC treatment. Meanwhile, 11 of 16 primary cells underwent apoptosis (Fig. 1A and B, Supporting Information Fig. S1A and S1B). These preliminary results lead to further research to determine whether MSC treatment holds the possibility of shaping the fate of acute myeloid leukemia cells.

To evaluate the exact effect of MSC treatment on AML cells, U937 and THP-1 cells were co-cultured with MSC. We observed irregularly shaped nuclei, an extended cytoplasm and the appearance of fine granules (Fig. 1C). Meanwhile, increased expression levels of CD14 and CD11b were observed (Fig. 1D and Fig. S1C), which was in agreement with the data obtained from the abovementioned primary AML cell experiments. Interestingly, the phagocytic activity of U937 and THP-1 cells after co-culturing was profoundly enhanced (Fig. 1E). The differentiation of AML cells was also revealed by assaying changes in the expression of myeloid genes, such as *CD71*, *CD68*, *CD14* and *CD11b* (Fig. 1F). In addition, MSC induced G0/G1 cell cycle arrest and apoptosis in U937 and THP-1 cells (Fig. 1F−H, Fig. S1D and S1E). Our preliminary findings demonstrated that MSC treatment mediated AML cell differentiation and conferred these aberrant blood cells with monocyte-like phenotypes.

3.2. MSC generates EVs to initiate the AML cell differentiation

Next, we sought to investigate the machineries involved in MSC-mediated AML cell differentiation. The MSC in Transwell co-culture system showed similar pro-differentiation efficacy with that in cell−cell contact co-culture system (Supporting Information Fig. S2A), which indicated that the MSC generated soluble mediators for triggering AML cell transformation. To explore the mediators that elicited this effect, we fractionated the components in the MSC culture supernatant (MSC-CM) and evaluated their efficacy on AML cells. First, the fraction containing the factors whose molecular size was lower than 3 kDa (<3 kD), failed to increase the number of $CD14^+CD11b^+$ cells, suggesting that MSC-derived small molecules had little impact on inducing AML cell differentiation. In contrast, the fraction (>3 kD) significantly augmented the expression of both CD14 and CD11b in U937 and THP-1 cells (Fig. S2B), which proved that certain pro-differentiation protein components existed in MSC-CM. Next, we performed the ultracentrifugation of the >3 kDa fraction and found that the pellets containing EVs showed more robust pro-differentiation effect on AML cells than that induced by supernatants containing cytokines (Fig. S2C). Electron microscopy evaluation confirmed the morphology and diameter of EVs (Fig. 2A). The biomarkers of EVs were tested by Western blotting (Fig. 2B). The internalization of EVs into AML cells was visualized by confocal microscopy (Fig. 2C). To verify the efficacy of EVs from MSC on AML cell differentiation, we treated U937 and THP-1 cells with purified EV particles. As shown in Fig. 2D and Fig. S2D, this treatment dramatically promoted AML cell differentiation in a dose-dependent manner. In contrast, impeding the formation and release of EVs by Y27632, an inhibitor of EV trafficking, impaired the pro-differentiation capacity of MSC (Fig. 2E and Fig. S2E). These results suggest that MSC released EVs to promote AML cell differentiation. Next, we tested the p38 MAPK−STAT3 signaling in AML cells, which has been reported as an important signaling pathway in hematopoietic cell differentiation[12,13]. The data shown that both U937 and THP-1 cells treated with MSC-EVs exhibited enhanced the phosphorylation levels of p38 MAPK and STAT3 (Fig. 2F, Fig. S2F and S2G). Cells treated with specific inhibitors of p38 MAPK (SB239063) or STAT3 (Stattic) inhibited EV-induced $CD14^+CD11b^+$ cell generation, meanwhile the combined treatment completely blocked the effect of EVs on AML cell differentiation (Fig. 2G, Fig. S2H and S2I). These data indicate that MSC-EVs promote AML cell differentiation *via* activating p38−STAT3 signaling.

To evaluate the anti-AML effect of MSC-EVs *in vivo*, AML mice were treated with 1×10^6 MSC and equivalent MSC-derived EVs. By evaluating human $CD45^+$ cells in peripheral blood (PB) and bone marrow (BM), we found that MSC and MSC-EVs showed similar effects on the reduction of the leukemia burden (Fig. 2H and I). Notably, a markedly higher level of differentiation was observed in both MSC- and MSC-EV-treated groups, as evidenced by the upregulation of the differentiation marker CD14 (Fig. 2J and K). Furthermore, significant attenuations of splenic infiltration were

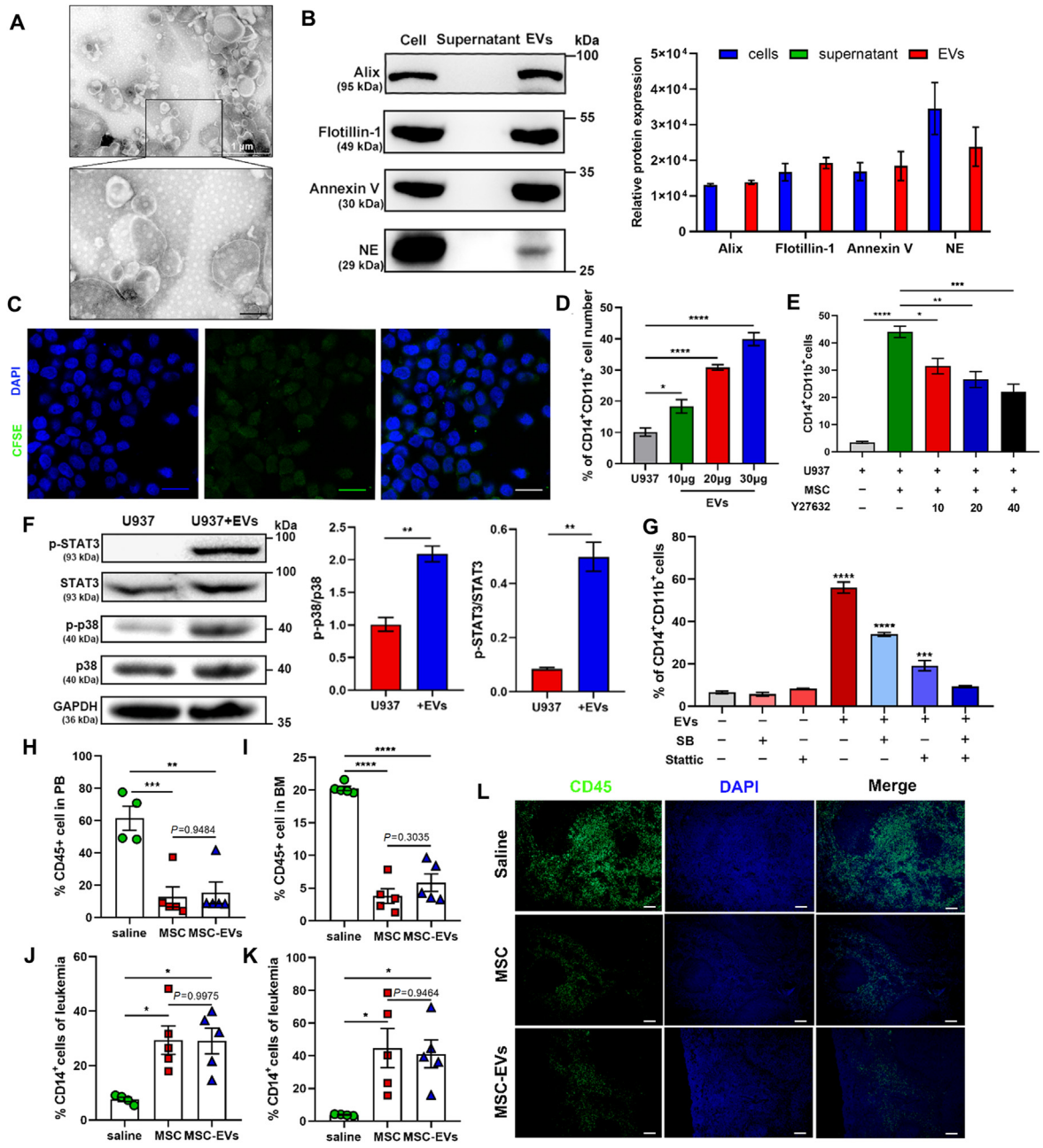

Figure 2 MSC promotes AML cell differentiation by EVs. (A) Electron microscopy image of EVs isolated from the conditional medium of MSC. Scale bar = 200 nm. (B) Western blotting for the expression of Alix, Flotillin-1, Annexin V and NE in MSC, supernatant and EVs which were extracted from MSC conditional medium, respectively. Data are quantified on the right. (C) Confocal microscopy images of U937 cells treated with EVs derived from CFSE-labelled MSC for 2 h. 100 × magnification; scale bar = 20 μm; (D) U937 cells were cultured with EVs (10, 20, and 30 μg) for 48 h. The myeloid differentiation markers CD11b and CD14 in U937 cells were analyzed by flow cytometry ($n = 3$). (E) U937 cells were cultured with MSC in the presence of EVs trafficking inhibitor Y27632 (10, 20, and 40 μmol/L) for 48 h. The myeloid differentiation markers CD11b and CD14 in U937 cells were analyzed by flow cytometry ($n = 3$). (F) MSC EVs (30 μg) were added to stimulate U937 cells. Western blotting was applied to detect the levels of phosphorylation of p38 and STAT3 in U937 cells. Data are quantified on the right. (G) U937 cells were treated by the p38 MAPK inhibitor SB239063 (SB) (10 μmol/L) and/or the STAT3 inhibitor Stattic (5 μmol/L) followed by incubating with MSC for 48 h. The percentage of $CD14^+CD11b^+$ cells was determined by flow cytometry. (H, I) Flow cytometry analysis of the percentage of leukemic cells (CD45 positive cells) in peripheral blood (PB) (I) and bone marrow (BM) (J) in vehicle, MSC-treated and MSC-EVs-treated mice after 25 days of transplantation ($n = 4$ or 5 each group). (J, K) Flow cytometry analysis of the expression of the differentiation marker CD14 in PB (K) and BM (L) derived leukemic cells ($n = 4$ or 5 each group). (L) Fluorescent images of the AML cells infiltration in the spleen as observed *via* immunofluorescence with anti-CD45 antibody (green). Nuclei are stained with DAPI (blue). 10 × magnification; scale bar = 100 μm. Data are expressed as the mean ± SEM. Data were analyzed by Student's *t* test (E, F) and one-way ANOVA followed by Tukey's test (D, G−K). $^*P < 0.05$, $^{**}P < 0.01$, $^{***}P < 0.001$, $^{****}P < 0.0001$.

shown in both MSC- and MSC-EV-treated mice (Fig. 2L). These findings suggest that MSC initiated AML cell differentiation *via* EVs, and that MSC-EVs exerted comparable effects to those of MSC.

3.3. Identification of neutrophil elastase (NE) is the key effector in MSC-EVs

To identify the specific components that determined the monocytic fate, we conducted secretome of MSC. MSC were pretreated with U937 cells in a Transwell system for 24 h, leukemic cells were removed, and the serum-free fresh culture media was changed for 48 h. The concentrated culture media was subjected to quantitative proteome analysis (Supporting Information Fig. S3A). As a result, a total of 28 upregulated proteins and 2 downregulated proteins were considered to be significantly changed proteins (defined as a P value < 0.05 and $\log_2(FC) > 1$) (Fig. 3A). To further narrow the scope of functional factors, we set up a higher threshold [$\log_2(FC) > 1.5$] for filtering the upregulated proteins, and obtained 14 candidates. Quantitative RT-PCR (qRT-PCR) assay demonstrated that, among these candidates, *ELANE* known as neutrophil elastase (NE) exhibited the highest induction level (>25-fold) of gene expression (Fig. S3B) when cocultured with U937 cells. Parallelly, in the co-culturing system, NE protein was specifically enriched in MSC but not in differential U937 cells (Fig. 3B and Fig. S3C). Previous studies have proven that NE abundance was positively correlated with the neutrophil differentiation[14,15]. According to TCGA datasets, AML patients with higher expression of NE showed an improved overall survival time (Fig. S3D). GEO dataset mining was also used to analyze the relationship between AML and NE expression. Weighted gene co-expression network analysis across samples from M0−M7 myeloid leukemia patients showed that *NE* gene was grouped into the blue module in which genes were negatively correlated with the M5 leukemia (monocytic leukemia) characteristics (Fig. 3C and D). The subsequent GO cluster confirmed that the genes in the *NE* grouped in the blue module were correlated with the leukocyte differentiation (Fig. S3E). The comprehensive bioinformatic analysis indicated that the NE expression level was highly linked to monocytic leukemia phenotype. Thus, these data suggest that NE might be a key factor in MSC-mediated AML cell differentiation.

Considering NE was detected in MSC-EVs (Fig. 2B), we speculated that MSC-EVs delivered NE to AML cells to initiate differentiation. To verify this hypothesis, we overexpressed the GFP (green fluorescence protein) fusion NE protein in MSC, collected secreted EVs and added them to recipient AML cells. Microscopy imaging and immunoblotting showed that EVs with NE cargo were internalized by leukemic cells (Fig. 3E). Furthermore, EVs from NE-overexpressed the MSC boosted both CD14 and CD11b expressions in U937 and THP-1 cells (Fig. 3F and Fig. S3F), accompanied by an enhancement of phagocytic activity (Fig. 3G and Fig. S3G). In contrast, the NE knockout (NE-KO) MSC generated EVs lost their pro-differentiation capacity (Fig. 3H, I, Fig. S3H and S3I). These data suggest that NE was the pivotal factor in MSC-EVs. Moreover, NE-induced differentiation of AML cells was significantly decreased by the NE inhibitor sivelestat (Fig. S3J and S3K), indicating that the activity of NE was requisite to promote AML cell differentiation. Given that NE is reported to regulate p38−STAT3 signaling pathways[16,17], we tested the effects of NE on the activation of this pathway. Treatment of U937 cells with NE for 2, 6, and 12 h resulted in a time-dependent increase in the phosphorylation levels of p38 MAPK and STAT3 (Fig. 3J). Specific inhibition of NE and p38 significantly diminished the phosphorylation of p38 and STAT3, respectively (Fig. 3K). These results indicate that NE propelled AML cell differentiation in p38/STAT3-dependent manner. Taken together, NE was the key effector in MSC-EVs which initiated AML cell differentiation.

3.4. VDR drives NE-loaded EVs production and controls the pro-differentiation ability in MSC

In light of the dramatic performance of MSC on AML cell differentiation, we wondered the molecular controller for this effect in MSC. We applied the upregulated differentially expressed proteins of U937-treated MSC in secretome to ChIP-X enrichment analysis. This analysis method enriched transcription factors (TFs) that drove the expression of these proteins, and vitamin D receptor (VDR) was identified as the most potential TF in controlling the MSC secretion behavior (Supporting Information Fig. S4A). To test the transactivation function of VDR on *NE* gene, we constructed a reporter gene system in which a luciferase gene was under a *NE* promoter (elane-luc). Following the treatment of 1,25D3, the natural VDR full agonist, VDR showed robustly enhanced activation in *NE* gene transcription, which verified that VDR was the upstream TF for NE expression (Fig. 4A). Consistent with the luciferase assay, agonism of VDR led to an increase of NE protein level in MSC (Fig. 4B and C). Meanwhile, greater transcriptional activity of VDR was observed in the combination of 1,25D3 and U937 cells (Fig. S4B). Further, to confirm the critical role of VDR in NE expression, the VDR knockdown (MSC&shVDR) and VDR-overexpressing MSC (MSC OE-VDR) were generated (Fig. S4C and S4D). Upon treatment with 1,25D3, MSC&shVDR dramatically impeded the *NE* expression (Fig. 4D). In contrast, this treatment highly enhanced the *NE* level in MSC OE-VDR (Fig. 4E). These data demonstrate that VDR was the transcriptional controller of *NE* in MSC. Next, we evaluated whether VDR activation could elevate the NE-packaged EV release of MSC and strengthened the AML cell differentiation. MSC were primed with 1,25D3, then, MSC-EVs were collected and added into U937 cells. As shown in Fig. 4F, 1,25D3-treated MSC generated more NE-packaged EVs into the supernatant. Moreover, EVs from 1,25D3-treated MSC exhibited a more marked pro-differentiation capacity on AML cells than EVs from untreated MSC (Fig. 4G and Fig. S4E). In contrast, VDR knockdown in MSC inhibited 1,25D3-induced EV production (Fig. 4H). To further validate the role of VDR in MSC-EV-mediated AML cell differentiation, VDR knockout MSC (MSC VDR-KO) were applied to the related cell experiments (Fig. S4F). VDR deletion in MSC completely blocked NE generation (Fig. S4G). Moreover, EVs from MSC VDR-KO showed impaired efficiency on AML differentiation (Fig. 4I). Collectively, these data demonstrate that the secretory action of NE-packed EVs in MSC was controlled by VDR.

In our previous work, we have noted that AML cells from myelomonocytic and monocytic AML patients expressed higher levels of IFN-γ and TNF-α than that from normal people. Notably, when co-culture with MSC, AML cells significantly enhanced the expressions of TNF-α and IFN-γ while MSC did not have this phenomenon[18]. Here, to explore the inducers for VDR activation, MSC were treated with recombinant IFN-γ or TNF-α and the *VDR* level was analyzed. As shown in Fig. S4H, TNF-α treatment significantly enhanced the *VDR* expression while IFN-γ did not. Consistent with *VDR* enhancement, the *NE* expression was also

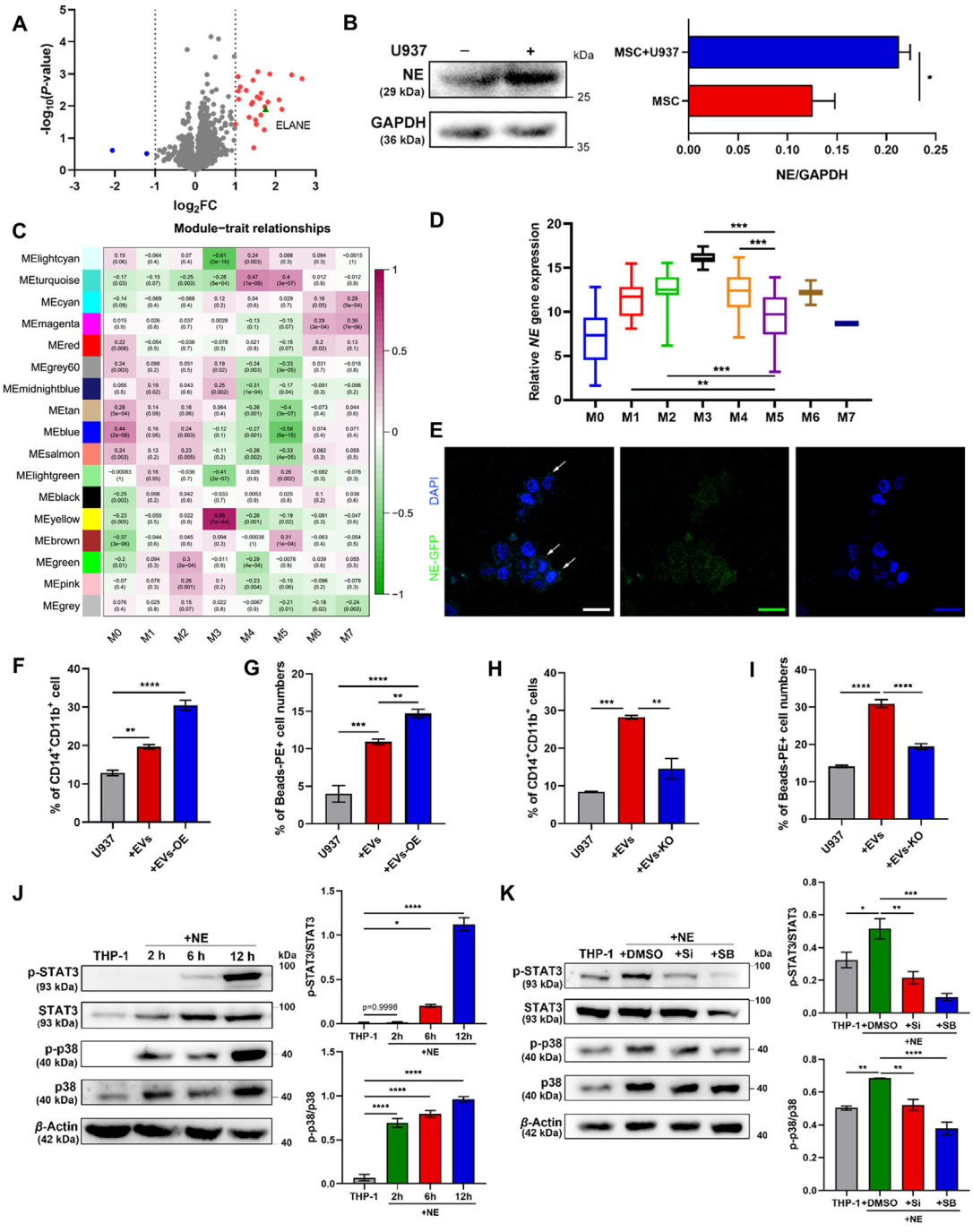

Figure 3 NE-packaged EVs are the key effector in MSC-mediated AML cell differentiation. (A) The volcano plot of differentially expressed proteins. Blue dots represented significantly down-regulated expression proteins. Red dots represented significantly up-regulated expression proteins. Green dot represented ELANE (defined as a P value < 0.05 and $\log_2(FC) > 1$). (B) Western blotting for the expression of NE in MSC upon the co-culture with or without U937 cells. Data are quantified on the right. (C) Weighted gene co-expression network analysis identified 16 modules with highly correlated gene expression patterns. Correlations between each module and the subtypes of AML (M0−M7) genotypes are shown by the intensity of the purple or green color. The P value for each module is shown in brackets. (D) *NE* expression levels of AML M5 samples and other subtypes of AML samples in TCGA datasets. (E) Confocal microscopy images of U937 cells treated with MSC EVs carrying GFP-labelled NE for 2 h. 100× magnification; scale bar = 20 μm. (F, G) EVs isolated from MSC CM or MSC OE-NE CM were added to U937 cells. The percentage of $CD14^+CD11b^+$ cells (F) and phagocytosis activity (G) were evaluated by flow cytometry ($n = 3$). (H, I) EVs isolated from MSC CM or MSC NE-KO CM were added to U937 cells. The percentage of $CD14^+CD11b^+$ cells (H) and phagocytosis activity (I) were evaluated by flow cytometry ($n = 3$). (J) Western blotting analysis of the time course of NE effects on p38 MAPK and STAT3 activities. Data are quantified on the right. (K) U937 cells were treated with NE in the presence or absence of the NE inhibitor Sivelestat (Si) (5 mmol/L) or SB239063 (SB) (10 μmol/L). Western blotting was applied to detect the levels of phosphorylation of p38 and STAT3 in U937 cells. Data are quantified on the right. Data are expressed as the mean ± SEM. Data were analyzed by Student's t test (B) and one-way ANOVA followed by Tukey's test (F)−(K). $^*P < 0.05$, $^{**}P < 0.01$, $^{***}P < 0.001$, $^{****}P < 0.0001$.

elevated in MSC upon TNF-α treatment (Fig. S4I). Parallelly, TNF-α expression in U937 cell and MSC were analyzed, and we found that the protein expression of TNF-α was significantly elevated in U937 cells when they were co-cultured with MSC (Fig. S4J), whereas no significant changes in TNF-α expression were found in MSC (Fig. S4K), indicating TNF-α was secreted by AML cells. These data suggest that TNF-α secreted by AML cells is a functional activator to induce VDR expression in MSC.

3.5. *Combined treatment with MSC and 1,25D3 synergistically promotes AML cell differentiation*

Given the tight link between VDR-driven EVs release and AML cell differentiation, we tried to construct the MSC-based therapy regimen. As MSC was able to persistently generate EVs, we speculated that the pharmacological activation of VDR would make MSC an ideal living drug for AML treatment. To test this speculation, U937 cells were treated with the combination of MSC and 1,25D3, and the differential markers were evaluated. Compared to the MSC group, the combinational treatment elicited a much higher expression of CD14 and CD11b (Fig. 5A and Supporting Information Fig. S5A), enhanced phagocytosis activity (Fig. 5B, Fig. S5B and S5C) and increased cell size in AML cells (Fig. 5C). The cell cycle was also analyzed, and we found that the combinational treatment reinforced the G0/G1 cell cycle arrest of U937 cells (Fig. 5D and Fig. S5D). These data suggest that the combination was more efficacious in inducing AML differentiation and that the prodifferentiative capacity of MSC could be improved by 1,25D3-mediated VDR activation. Moreover, the addition of 1,25D3 to the co-culture system increased the phosphorylation of p38 MAPK, and STAT3 in AML cells (Fig. S5E and S5F). Overall, our data demonstrate that 1,25D3 facilitated the enhancement of the pro-differentiation ability of MSC by activating VDR. On this basis, we developed a combination regimen of MSCs plus 1,25D3 for treating AML.

Since the above results resulted in a positive outcome for treatment with MSC plus 1,25D3 *in vitro*, we next extended our research to a mouse leukemia model. AML mice were treated with either 1,25D3 or MSC alone or in combination. Twenty-five days post-injection, MSC with/without 1,25D3 treated groups showed improved survival. The median survival was 34.5 days in the MSC-treated group, 31 days in the 1,25D3-treated group, 44 days in the combination-treated group and 26.5 days in the vehicle-treated group (Fig. S5G). Moreover, the administration of either agent substantially attenuated the weight of the liver and spleen (Fig. 5E and F) and reduced the leukemia burden in PB and BM compared to that in vehicle-treated mice (Fig. 5G and H). It is noteworthy that the leukemia burden of the combination-treated mice decreased to 5% in PB and 2% in BM, which was associated with a markedly higher level of differentiation than that associated with the single treatments (Fig. 5I and J). Furthermore, a further significant attenuation of splenic infiltration was shown in MSC/1,25D3-treated mice (Fig. 5K). Parallelly, the abundance of NE-packaged EVs was highly elevated in combination-treated mouse serum (Fig. S5H). These findings suggest that MSC/1,25D3 treatment indeed executes a synergistic pro-differentiation function in the mouse AML model and provide *in vivo* proof that combined treatment could increase the therapeutic efficacy in AML.

Additionally, to evaluate the safety of 1,25D3-treated MSC (pre-MSC), pre-MSC was monitored in adult male C57BL/6 mice after a single intravenous injection. The control group was given 100 μL of physiological saline per animal, and the treatment group received the same volume of a suspension containing MSC (10^8/kg). Seven days after the administration, normal hematological parameters and blood biochemical indexes were performed and no significant difference existed in the pre-MSC-treated group in comparison with the control group (Supporting Information Fig. S6A and S6B). Moreover, the histopathological analysis of the liver, spleen and kidney showed no obvious pathological alterations in pre-MSC-treated mice (Fig. S6C), suggesting that 1,25D3-modulated MSC treatment did not present potential toxicity. Taken together, our data highlight that 1,25D3-modulated MSC therapy was efficient and safe.

3.6. *A novel VDR agonist, sw-22, boosts the differentiation-promoting effect of MSC*

Although 1,25D3 exerts a marked anti-leukemia ability on AML cells, its potent calcemic activity, which results in hypercalcemia or hypercalciuria, is the major limiting factor in the clinical application[19]. To find potent VDR agonists with a reduced risk of increasing serum calcium, 108 nonsteroidal 1,25D3 analogues were designed and synthesized in our previous work[20–22]. Then, seven compounds were picked according to the analysis of their structure–activity relationships and their capacity for AML differentiation induction (Supporting Information Table S2). Among these, sw-22 was selected on account of its low cytotoxicity and its preferable ability to promote leukemia cell differentiation (Fig. 6A and B and Supporting Information Fig. S7A–S7D). After incubation with sw-22, MSC displayed dramatic increases in NE and EVs production (Fig. 6C, D and Fig. S7E), suggesting the enhancing effect of sw-22 on NE-packaged EVs generation in MSC. Considering that sw-22 is a VDR agonist, MSC & shVDR and sw-22 were used to treat U937 cells. As expected, we found that MSC & shVDR exhibited reduced expression of NE, and the suppressed capacity on AML differentiation (Fig. 6E and F). Moreover, the application of sw-22 increased the phosphorylation of p38 MAPK, and STAT3 in co-cultured AML cells (Fig. S5F and S5G). Taken together, these findings demonstrate that sw-22 activated VDR to induce AML cell differentiation *via* facilitating the generation of NE-loaded EVs from MSC.

We next exploited a xenograft AML mouse model to evaluate the therapeutic effects of the sw-22 and MSC combination. Cytarabine (5 mg/kg), one of the most common AML clinical treatments, served as a positive control. The regimen of MSC/sw-22 resulted in dramatically prolonged survival compared with vehicle-treated mice (26 days) or mice treated with either MSC or sw-22 alone (33 days for MSC and 32 days for sw-22) and reached similar clinical outcomes with cytarabine treatment (38 days for cytarabine) (Fig. 6G). In addition, the combination-treated mice showed a remarkable reduction of leukemia burden in PB and BM compared to that in vehicle-treated mice (Fig. 6H, I and Fig. S7H). Histological analysis further confirmed the profoundly attenuated splenic and hepatic infiltration of leukemia cells (Fig. 6J). These data suggest that MSC/sw-22 treatment efficiently ameliorated the AML burden and executed a synergistic differentiation-promoting effect *in vivo*. Notably, a significant increase in CD14 and CD11b expressions were found in primary AML cells treated with MSC/sw-22 or the single treatments *ex vivo* (Fig. 6K, L and Fig. S7H), corroborating the effects on differentiation observed in the mouse AML model and the human AML cell lines. Taken together, our findings provide an efficient pro-differentiation therapeutic

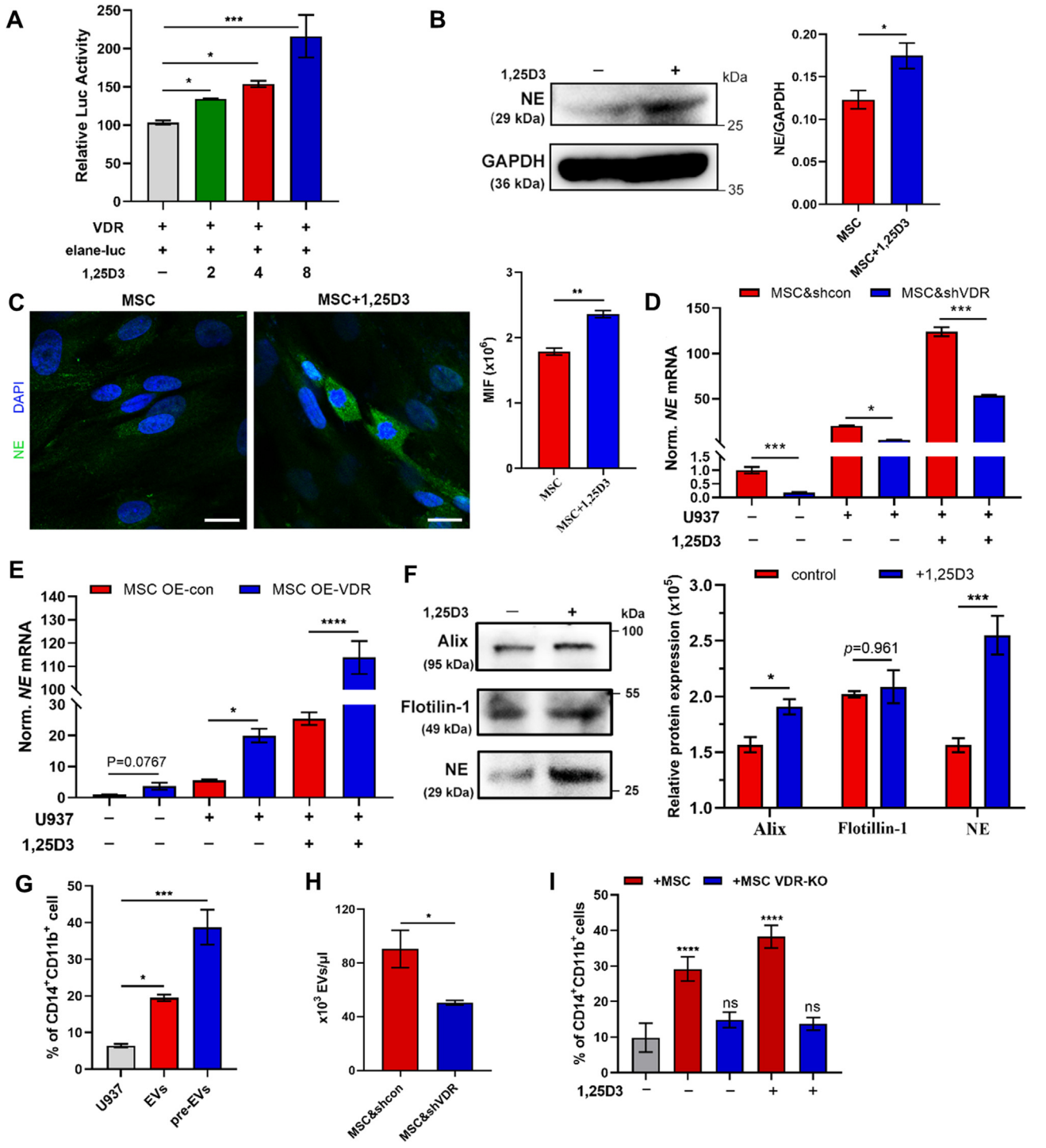

Figure 4 VDR modulates the production and release of NE carried EVs. (A) Luciferase reporter assay evaluating the transcriptional activity of VDR, following treatment with 1,25D3 ($n = 6$). (B) Relative NE protein level in DMSO- or 1,25D3-treated MSC was evaluated by Western blotting ($n = 3$). (C) Confocal microscopy analysis of the NE expression (Alexa Fluor 488) in DMSO- or 1,25D3-treated MSC. Data are quantified on the right. 100× magnification; scale bar = 20 μm. (D) The *NE* expressions in MSC & shcon or MSC & shVDR treated by U937 cells with or without 1,25D3 were assessed by RT-qPCR ($n = 3$). (E) The *NE* expression in MSC OE-con or MSC OE-VDR treated by U937 cells with or without 1,25D3 was assessed by RT-qPCR ($n = 3$). (F) MSC was cultured in the presence or absence of 1,25D3. The expressions of Alix, Flotillin-1, NE in MSC-EVs were detected by Western blotting ($n = 3$). Data are quantified on the right. (G) EVs isolated from 1,25D3-primed MSC (pre-EVs) were added to treat U937 cells. The myeloid differentiation markers CD11b and CD14 in U937 cells were analyzed by flow cytometry. ($n = 3$) (H) The numbers of EVs existed in MSC & shcon or MSC & shVDR medium were assessed by flow cytometry ($n = 3$). (I) U937 cells were treated by MSC or MSC VDR-KO in the presence with or without 1,25D3. The expressions of CD14 and CD11b in U937 cells were evaluated by flow cytometry ($n = 3$). All statistical data in this figure are expressed as the mean ± SEM. Data were analyzed by Student's *t* test (B, C), two-way ANOVA followed by Bonferroni's test (D, E, F, I) and one-way ANOVA followed by Tukey's test (B, C, H). $^{*}P < 0.05$, $^{**}P < 0.01$, $^{***}P < 0.001$, $^{****}P < 0.0001$.

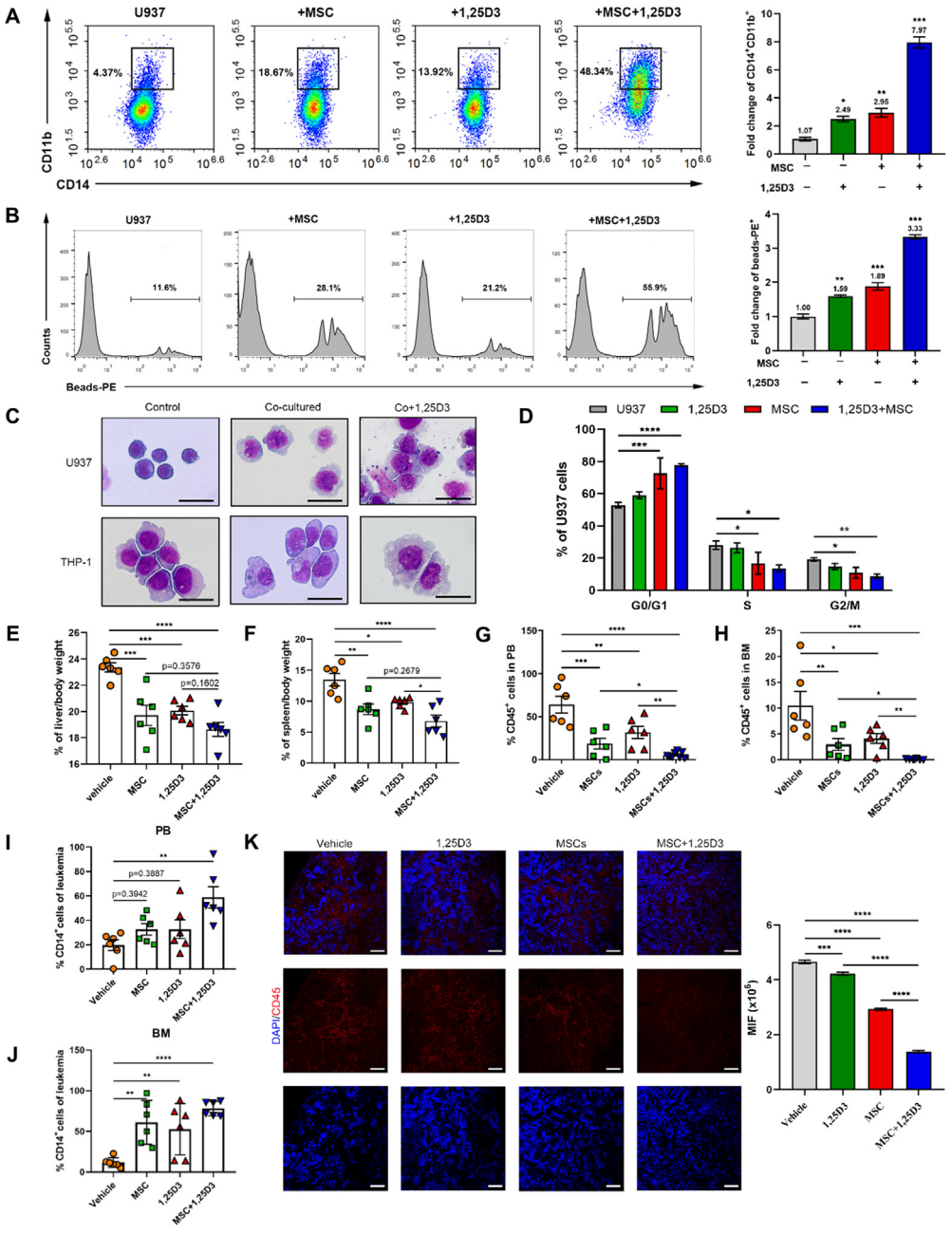

Figure 5 VDR activation enhances MSC-mediated pro-differentiation effect on AML cells. (A, B) U937 cells were cultured alone or incubated with MSC in the presence or absence of 1,25D3 (8 nmol/L) for 48 h. The differentiation markers CD14 and CD11b (A), phagocytosis activity (B) in U937 cells were measured by flow cytometry. Fold increase of CD14 and CD11b expressions and phagocytosis beads (mean fluorescence intensity relative to untreated cells) were quantified on the right ($n = 3$). (C) Morphological changes were confirmed by Wright−Giemsa staining of cells with or without MSC and 1,25D3 culture. Scale bar = 25 μm. (D) U937 cells were cultured alone or incubated with MSC in the presence or absence of 1,25D3. Flow cytometry analysis of cell cycle of U937 cells ($n = 3$). (E, F) The weight index of liver (E) and spleen (F) in different groups ($n = 6$). (G, H) Flow cytometry analysis of the percentage of leukemic cells in PB (G) and BM (H) in vehicle, single agent-treated and combination-treated mice after 25 days of transplantation ($n = 6$). (I, J) Flow cytometry analysis of the expression of the differentiation marker CD14 in PB (I) and BM (J) derived leukemic cells ($n = 6$). (K) Fluorescent images (left) and quantitation (right) of the AML cells infiltration in the spleen as observed *via* immunofluorescence with anti-CD45 antibody (red). Nuclei are stained with DAPI (blue). Scale bar = 75 μm. A dot depicts data from an individual animal, and all the histograms in this figure show the mean ± SEM. Data were analyzed by two-way ANOVA followed by Bonferroni's test (D) or one-way ANOVA followed by Tukey's test (A, B, E−K). $^{*}P < 0.05$, $^{**}P < 0.01$, $^{***}P < 0.001$, $^{****}P < 0.0001$.

strategy, MSC/sw-22 treatment, to ameliorate the AML burden without hypercalcemia (Fig. S7I).

4. Discussion

For AML treatment, high-dose chemotherapy combined with HSCT is considered the most commonly used clinical approach. Despite the fact that this combinatorial strategy achieves complete remission for many patients, intensive chemotherapy often produces intolerable adverse effects[23,24]. In addition, patients undergoing HSCT have been shown to be at a high risk of infection and post-transplantation disease relapse[25]. Recently, anti-CD19/CD20 CAR-T cells have become available in clinical practice for treating B-cell acute lymphoblastic leukemia and non-Hodgkin lymphoma, which has brought new hope to patients with blood malignancies[26,27]. However, current CAR-T therapies designed for AML have failed in clinical trials due to the lack of ideal specific surface antigens, which causes severe damage to normal myeloid cells[28]. These disappointing outcomes indicate the need for the further development of alternative effective therapeutic strategies. For this purpose, we attempted to design a cellular therapy for treating AML in our preliminary investigation and found that UC-MSC transplantation effectively controlled AML progression. Thus, in the current study, we provided a non-gene editing MSC-based anti-AML therapy regimen as a means to perform AML differentiation therapy. We demonstrated that MSC exhibited a significant differentiation-inducing effect on AML cells and remitted the progression of AML. Mechanistically, we discovered that the pro-differentiation capacity of MSC mainly leaned upon transmitting NE-loaded EVs generated by MSC into AML cells. Further, VDR activation in MSC was proven to impel the production and secretion of NE-loaded EVs. Notably, chemical activation of VDR using its agonists markedly increased NE-packaged EV production in MSC, and exerted synergetic enhancement effects with MSC on alleviating AML burden (Fig. 6M). The anti-leukemic activity of the combinatorial regimen may offer a promising therapeutic option for AML treatment.

MSC are essential mediators in the maintenance and regulation of hematopoiesis and immune system homeostasis[29]. Nevertheless, several clinical investigations pointed out that, in blood malignancies, patient-derived MSC were functionally impaired in specifically supporting leukemic cells over normal HSCs[30−32], and aggravating disease progression. Considering these discoveries, we postulated whether allogeneic MSC treatment could remedy the deficiency displayed by autologous MSC. As expected, allogeneic UC-MSC transplantation significantly alleviated the AML burden and prolonged the survival period in a mouse model. Importantly, we made an exciting observation that UC-MSC mediated AML cell differentiation by instructing them to acquire mature monocyte-like features. Retrospective drug utilization manifests that only retinoic acid and arsenic have been successfully used to promote leukemic cell differentiation in curing acute promyelocytic leukemia[33]. There is still a lack of effective pro-differentiation methods for inducing the differentiation of primary AML cells from other subtypes of AML. Here, we collected 27 primary blood samples from AML-M4/M5 patients, and 80% of the sample cells underwent differentiation upon UC-MSC treatment. Despite that UC-MSC infusion has not been approved in AML patients, the partial achievement of primary AML cell differentiation in our study hinted that MSC might serve as an approach to treat AML by overcoming their blocked differentiation.

We found that UC-MSC first mediated AML cell differentiation *via* secreted EVs. To address the underlying mechanism, we used a combination strategy that included quantitative proteomic techniques and specific bioinformatics analysis. We further identified NE as a major bioactive factor packaged in MSC-EVs, which shuttled into AML cells and initiated the differentiation of AML cells. Inhibiting EVs release or knocking out the NE gene significantly impaired the pro-differentiation effect of MSC, suggesting that NE-loaded EVs played a prominent role in MSC-mediated AML cell differentiation. EVs play a crucial role in mediating cell-to-cell communication. Recent studies have demonstrated that EVs from MSC (MSC-EVs) shuttled important bioactive molecules between cells, and influenced physiological or pathological process[34,35]. These EVs exhibited various therapeutic actions on tissue regeneration and inflammatory regulation[36,37]. Compared to MSC treatment, the application of MSC-EVs takes several advantages such as higher safety, lower immunogenicity and the capacity to cross biological barriers[38−40]. These advantages have sparked intensive research into developing MSC-EVs-based therapeutic regimen for treating refractory diseases. Despite the success in MSC-EVs treatment in preclinical studies, the cargo components in MSC-EVs that mediate the communication between MSC and target cells have not been clearly dissected. A comprehensive study elucidated that NE was an effective anti-cancer factor which killed cancer cells with minimal toxicity to non-cancer cells[41]. Our results, for the first time, pointed out that NE promoted AML cell differentiation by activating p38−STAT3 signaling, an important pathway that is involved in regulating hematopoietic cell differentiation. This finding indicated that NE was a kind of pleiotropic antitumor factor. Notably, we found that NE-packaged MSC-EVs exerted comparable effects to MSC on inducing AML cell differentiation and improving AML progression (Fig. 2), which suggested that NE-packed MSC-EVs were essential in MSC-mediated AML cell differentiation.

Our *in vitro* data demonstrate that MSC incubating with AML cells significantly up-regulated the VDR expression. This phenomenon hinted that AML cells might secrete some unknown bioactive factors to stimulate the VDR expression in MSC. Previous studies have shown that inflammatory cytokines, such as IFN-γ and TNF-α, secreted by leucocytes possessed the ability in regulating VDR abundance and activity[42,43]. In our previous study, we found AML cells from myelomonocytic and monocytic AML patients expressed higher levels of IFN-γ and TNF-α than that from normal people. AML cells incubating with MSC significantly enhanced the expressions of TNF-α and IFN-γ[18]. Accordingly, in this study, the VDR activation upon TNF-α or IFN-γ treatment was detected. TNF-α significantly enhanced the VDR expression while IFN-γ did not. Collectively, these findings indicated that TNF-α secreted by AML cells is a functional activator to induce VDR expression in MSC.

It is noteworthy that we have obtained an intriguing achievement that VDR activation dramatically enhances the anti-AML effects of MSC, revealing a novel function of VDR acting as an upstream regulator of NE in MSC. To date, studies of VDR in MSC have been restricted to its regulatory function in osteogenic differentiation[44]. The role played by VDR in other biological behaviors of MSC is largely unknown. We found, for the first time, a specific role of VDR in MSC secretory function and linked the EVs interaction to AML cell differentiation. In addition, VDR

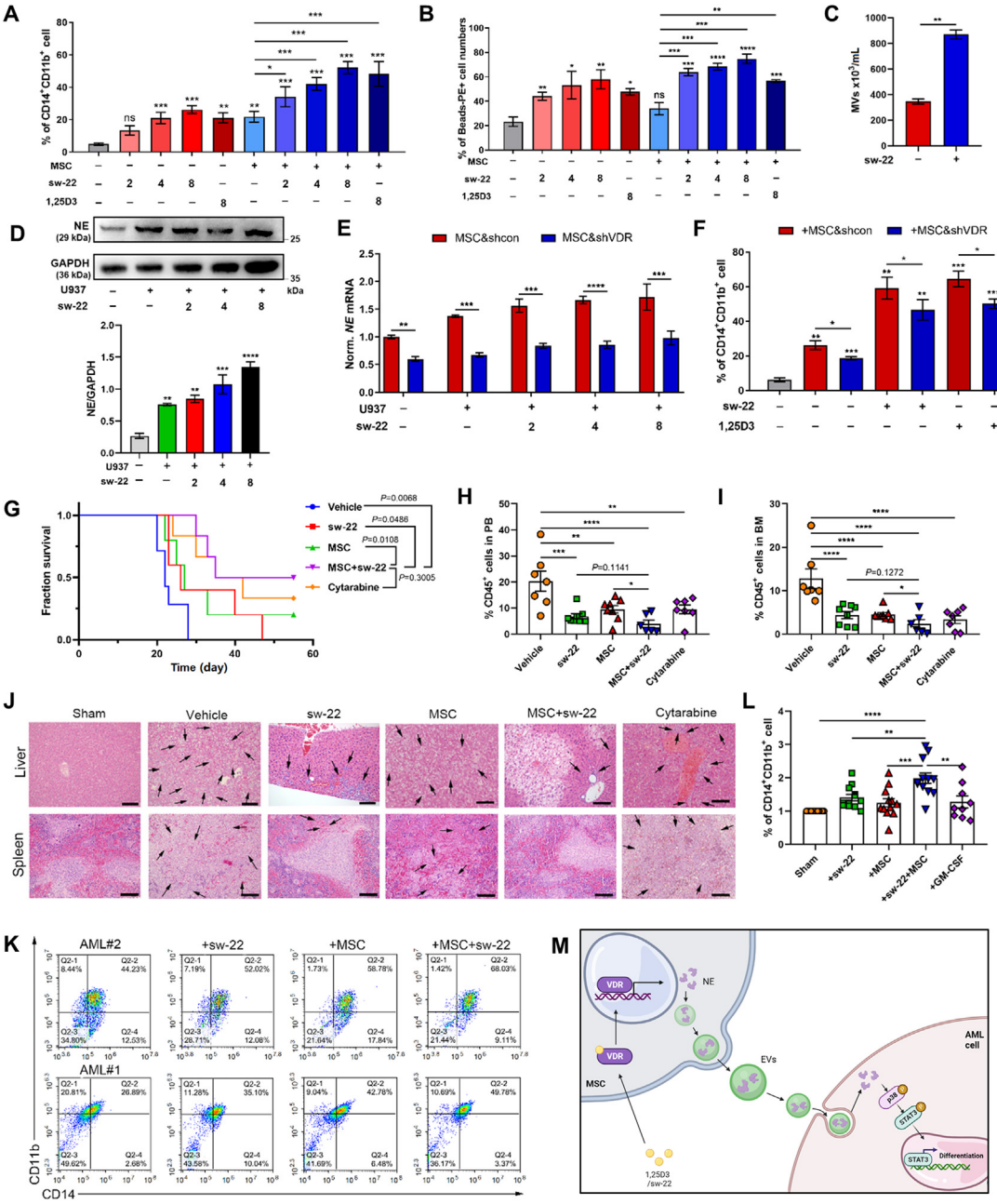

Figure 6 Sw-22 combined with MSC synergistically played an anti-leukemia effect without hypercalcemia. (A, B) U937 cells were cultured alone or cocultured with MSC in the presence or absence of different doses of sw-22 (2, 4, and 8 μmol/L) for 48 h, 1,25D3 (8 nmol/L) was applied as positive control. The differentiation markers CD14 and CD11b (A) and phagocytosis (B) were measured by flow cytometry ($n = 3$). (C) Flow cytometry assessed the numbers of EVs existed in sw-22-treated MSC ($n = 3$). (D) Western blotting for the expression of NE in MSC treated by U937 cells combined with different doses of sw-22 (2, 4, and 8 μmol/L). Data are quantified below. (E) MSC & shcon or MSC & shVDR were cultured alone or cocultured with U937 cells in the presence or absence of different doses of sw-22. The expression of *NE* in MSC & shcon or MSC & shVDR was assessed by RT-qPCR ($n = 3$). (F) U937 cells were treated with MSC & shcon or MSC & shVDR in the presence or absence of sw-22 for 48 h. Flow cytometry analyzed the CD14 and CD11b expressions. ($n = 3$) (G) Survival curves of AML recipient mice treated with vehicle, sw-22, MSC, sw-22 plus MSC or cytarabine. Mice treated with the combination treatment showed prolonged survival. (H, I) Flow cytometry analysis of the percentage of leukemic cells in PB (H) and BM (I) of vehicle, single agent-treated and combination-treated mice after 25 days of transplantation ($n = 6$ or 7 per group). (J) Histologic sections of spleen were stained with hematoxylin−eosin (HE). Scale bar = 100 μm. (K) $CD11b^+CD14^+$ cells in primary human cells from AML-M5 patients after combination stimulation. (L) $CD11b^+CD14^+$ cells in primary human cells from FAB M4 and M5 patients after single-agent or combination treatment ($n = 9$ or 10 per group). (M) Graphical illustration of the interaction between MSC and AML cells. All statistical data in this figure are expressed as the mean ± SEM. Data were analyzed by two-way ANOVA followed by Bonferroni's test (E, F) or one-way ANOVA followed by Tukey's test. $^*P < 0.05$, $^{**}P < 0.01$, $^{***}P < 0.001$, $^{****}P < 0.0001$.

has been demonstrated to be an important regulator in AML cells of the induction of leukemic cell differentiation[45]. Therefore, the coregulation of VDRs in MSC and AML cells using chemical compounds is a promising strategy for promoting AML cell differentiation. In fact, chemical modulation or reprogramming has been shown to be an efficient and safe approach to control the variability and functionality of stem cells, which avoids the potential health risks of gene editing in humans[46]. In addition, the quality control of small chemical molecules used for stem cell modulation is far easier than that of conventional virus-mediated gene delivery methods[47]. For example, the full chemical induction of induced pluripotent stem cells has been realized by utilizing a cocktail of seven small molecules[48]. Similarly, kartogenin, a small chemical molecule that targets the FLNA−CBFβ interaction in MSC, induced MSC-chondrocyte differentiation at local sites and stimulated the repair of damaged cartilage in osteoarthritis models[49]. Here, we successfully activated VDR in MSC *via* a single chemical small molecule, 1,25D3, which further enhanced the pro-differentiation capacity of MSC.

However, 1,25D3 is a secosteroid structure (natural structure) VDR agonist, this traditional secosteroid structure also makes 1,25D3 have a strong affinity to vitamin D binding protein (DBP), a major transport protein in serum for all vitamin D metabolites[50]. The 1,25D3−DBP complex strongly activates the calcium metabolism-related signaling pathway in the intestine and promotes the absorption of calcium ions from diets, which leads to the dramatical up-regulation of the concentration of blood calcium (hypercalcemia)[19]. In clinic, 1,25D3 led to life-threatening hypercalcemia in 20%−30% of human patients; thus, its clinical trials in the treatment of AML were interrupted[51]. To avoid the adverse effects of VDR agonists in clinical regimens, novel vitamin D receptor modulators were needed. Thus, the idea of developing nonsteroidal VDR agonists was raised, and these nonsteroidal analogues, such as LG190155, possessed low affinity to DBP and did not induce hypercalcemia[52,53]. Based on the structural backbone of LG190155, we designed a series of nonsteroidal VDR agonists to further enhance the compound stability and activity in our previous work. By screening the activity, we picked out TOP 7 compounds to be used in the present study and sw-22 exhibited the highest efficiency to enhance the pro-differentiation effect of MSC. Notably, sw-22 did not induce a significant increase in serum calcium in an animal model. These findings identified sw-22 as a safe drug candidate for a combinational therapeutic strategy with MSC for treating AML.

In summary, our findings demonstrate that allogeneic UC-MSC from healthy donors confer monocytic differentiation properties on AML cells by functioning as a cellular therapeutic tool for combating AML. Most importantly, our results reveal the critical role of VDR activation in the expression of NE in MSC. This interaction reinforces the release of EVs to enhance the pro-differentiation effect of MSC on leukemia cells. Furthermore, by using cell-based phenotypic screening, we identify a molecular probe, 1,25D3, that activates the VDR-NE interaction. The results not only suggest a novel function of 1,25D3 in the chemical modulation of MSC, but also reveal that VDR is an upstream regulator that controls the generation and release of NE-loaded EVs. Based on these discoveries, we also have identified sw-22, a novel nonsteroidal VDR modulator, as a promising activator of the VDR-NE interaction that has a strong impact on MSC-triggered AML cell differentiation but does not increase the level of serum calcium. Collectively, our findings provide a potential efficient pro-differentiation therapeutic avenue that can reduce the AML burden without hypercalcemia induction by the use of MSC reprogrammed by sw-22.

5. Conclusions

We established a novel stem cell-based regimen to AML differentiation therapy. By using the chemical activation of VDR in MSC, we successfully engineered MSC as the biogenerator for the production of EVs that can deliver a broad anti-tumor factor—NE to AML cells and promote leukemic cell differentiation. Our findings not only identified the novel function of VDR in MSC, but also provided a convenient approach to endow MSC to be a powerful living drug for AML therapy. In addition, by screening functional small molecules, we also provided an alternative VDR agonist for the chemical modulation of MSCs, which could avoid the potential side effect of 1,25D3 (natural VDR full agonist) in clinical use. Notably, compared to the gene editing strategy commonly used in stem cell programming, this stem cell-based regimen has no effect on genome stability, thus the quality and security control of this approach is far easier than that of conventional virus-mediated gene delivery methods. Collectively, our findings provide an efficient and safe pro-differentiation therapeutic tactic that ameliorated AML burden and offer the possibility of developing a non-gene editing MSC-based anti-AML therapy.

Acknowledgments

This work was supported by grants from the Natural Science Foundation of Jiangsu Province (BK20222009, China), Guangdong Basic and Applied Basic Research Foundation (2021B1515120016, China), National Natural Science Foundation of China (81972261), China Postdoctoral Science Foundation (2022M712436) and Zhejiang Provincial Natural Science Foundation of China under Grant No. LQ23H070001. This manuscript has been revised and polished by Nature Publishing Group.

Author contributions

Prof. Pingping Shen and Prof. Xiaokun Li conceived and supervised the project and wrote the manuscript. Prof. Weijian Sun designed the experiments and modified the manuscript. Luchen Sun and Nanfei Yang generated a large amount of data. Prof. Bing Chen and Prof. Peipei Xu provided and analyzed patients' samples. Nan Zhang provided transfection material. Yuncheng Bei conducted the bioinformatics experiments. Prof. Can Zhang and Zisheng Kang designed and synthesized the nonsteroidal VDR modulators. Prof. Yang Wei, Prof. Jia Wei and Prof. Jiangqiong Ke analyzed the data and gave technical support.

Conflicts of interest

The authors declare no conflicts of interest.

Appendix A. Supporting information

Supporting data to this article can be found online at https://doi.org/10.1016/j.apsb.2023.05.007.

References

1. Short NJ, Rytting ME, Cortes JE. Acute myeloid leukaemia. *Lancet* 2018;**392**:593−606.
2. Lo-Coco F, Avvisati G, Vignetti M, Thiede C, Orlando SM, Iacobelli S, et al. Retinoic acid and arsenic trioxide for acute promyelocytic leukemia. *N Engl J Med* 2013;**369**:111−21.
3. de Thé H. Differentiation therapy revisited. *Nat Rev Cancer* 2018;**18**:117−27.
4. Cornelissen JJ, Blaise D. Hematopoietic stem cell transplantation for patients with AML in first complete remission. *Blood* 2016;**127**:62−70.
5. Middeke JM, Fang M, Cornelissen JJ, Mohr B, Appelbaum FR, Stadler M, et al. Outcome of patients with abnl(17p) acute myeloid leukemia after allogeneic hematopoietic stem cell transplantation. *Blood* 2014;**123**:2960−7.
6. Shi W, Jin W, Xia L, Hu Y. Novel agents targeting leukemia cells and immune microenvironment for prevention and treatment of relapse of acute myeloid leukemia after allogeneic hematopoietic stem cell transplantation. *Acta Pharm Sin B* 2020;**10**:2125−39.
7. Zhu Y, Sun Z, Han Q, Liao L, Wang J, Bian C, et al. Human mesenchymal stem cells inhibit cancer cell proliferation by secreting DKK-1. *Leukemia* 2009;**23**:925−33.
8. Song N, Gao L, Qiu H, Huang C, Cheng H, Zhou H, et al. Mouse bone marrow-derived mesenchymal stem cells inhibit leukemia/lymphoma cell proliferation *in vitro* and in a mouse model of allogeneic bone marrow transplant. *Int J Mol Med* 2015;**36**:139−49.
9. Ramasamy R, Lam EW, Soeiro I, Tisato V, Bonnet D, Dazzi F. Mesenchymal stem cells inhibit proliferation and apoptosis of tumor cells: impact on *in vivo* tumor growth. *Leukemia* 2007;**21**:304−10.
10. Mizukami A, Thomé CH, Ferreira GA, Lanfredi GP, Covas DT, Pitteri SJ, et al. Proteomic identification and time-course monitoring of secreted proteins during expansion of human mesenchymal stem/stromal in stirred-tank bioreactor. *Front Bioeng Biotechnol* 2019;**7**:154.
11. de Araujo Farias V, O'Valle F, Serrano-Saenz S, Anderson P, Andres E, Lopez-Penalver J, et al. Exosomes derived from mesenchymal stem cells enhance radiotherapy-induced cell death in tumor and metastatic tumor foci. *Mol Cancer* 2018;**17**:122.
12. Ito K, Hirao A, Arai F, Takubo K, Matsuoka S, Miyamoto K, et al. Reactive oxygen species act through p38 MAPK to limit the lifespan of hematopoietic stem cells. *Nat Med* 2006;**12**:446−51.
13. Oh I-H, Eaves CJ. Overexpression of a dominant negative form of STAT3 selectively impairs hematopoietic stem cell activity. *Oncogene* 2002;**21**:4778−87.
14. Huang JY, Zhou QL, Huang CH, Song Y, Sharma AG, Liao Z, et al. Neutrophil elastase regulates emergency myelopoiesis preceding systemic inflammation in diet-induced obesity. *J Biol Chem* 2017;**292**:4770−6.
15. Duan Z, Li FQ, Wechsler J, Meade-White K, Williams K, Benson KF, et al. A novel notch protein, N2N, targeted by neutrophil elastase and implicated in hereditary neutropenia. *Mol Cell Biol* 2004;**24**:58−70.
16. Kuwahara I, Lillehoj EP, Lu W, Singh IS, Isohama Y, Miyata T, et al. Neutrophil elastase induces *IL-8* gene transcription and protein release through p38/NF-κB activation *via* EGFR transactivation in a lung epithelial cell line. *Am J Physiol Lung Cell Mol Physiol* 2006;**291**:L407−16.
17. Kuwahara I, Lillehoj EP, Koga T, Isohama Y, Miyata T, Kim KC. The signaling pathway involved in neutrophil elastase stimulated MUC1 transcription. *Am J Respir Cell Mol Biol* 2007;**37**:691−8.
18. Sun L, Wang J, Wang Q, He Z, Sun T, Yao Y, et al. Pretreatment of umbilical cord derived MSCs with IFN-γ and TNF-α enhances the tumor-suppressive effect on acute myeloid leukemia. *Biochem Pharmacol* 2022;**199**:115007.
19. Tebben PJ, Singh RJ, Kumar R. Vitamin D-mediated hypercalcemia: mechanisms, diagnosis, and treatment. *Endocr Rev* 2016;**37**:521−47.
20. Hao M, Hou S, Xue L, Yuan H, Zhu L, Wang C, et al. Further developments of the phenyl-pyrrolyl pentane series of nonsteroidal vitamin D receptor modulators as anticancer agents. *J Med Chem* 2018;**61**:3059−75.
21. Wang B, Hao M, Zhang C. Design, synthesis and biological evaluation of nonsecosteroidal vitamin D3 receptor ligands as anti-tumor agents. *Bioorg Med Chem Lett* 2017;**27**:1428−36.
22. Kang ZS, Wang C, Han XL, Du JJ, Li YY, Zhang C. Design, synthesis and biological evaluation of non-secosteriodal vitamin D receptor ligand bearing double side chain for the treatment of chronic pancreatitis. *Eur J Med Chem* 2018;**146**:541−53.
23. Zuckerman T, Ram R, Akria L, Koren-Michowitz M, Hoffman R, Henig I, et al. BST-236, a novel cytarabine prodrug for patients with acute leukemia unfit for standard induction: a phase 1/2a study. *Blood Adv* 2019;**3**:3740−9.
24. Crossnohere NL, Richardson DR, Reinhart C, O'Donoghue B, Love SM, Smith BD, et al. Side effects from acute myeloid leukemia treatment: results from a national survey. *Curr Med Res Opin* 2019;**35**:1965−70.
25. Granot N, Storb R. History of hematopoietic cell transplantation: challenges and progress. *Haematologica* 2020;**105**:2716−29.
26. Chow VA, Shadman M, Gopal AK. Translating anti-CD19 CAR T-cell therapy into clinical practice for relapsed/refractory diffuse large B-cell lymphoma. *Blood* 2018;**132**:777−81.
27. Shah NN, Johnson BD, Schneider D, Zhu F, Szabo A, Keever-Taylor CA, et al. Bispecific anti-CD20, anti-CD19 CAR T cells for relapsed B cell malignancies: a phase 1 dose escalation and expansion trial. *Nat Med* 2020;**26**:1569−75.
28. Mardiana S, Gill S. CAR T cells for acute myeloid leukemia: state of the art and future directions. *Front Oncol* 2020;**10**:697.
29. Ko JH, Kim HJ, Jeong HJ, Lee HJ, Oh JY. Mesenchymal stem and stromal cells harness macrophage-derived amphiregulin to maintain tissue homeostasis. *Cell Rep* 2020;**30**:3806−38020.e6.
30. von der Heide EK, Neumann M, Vosberg S, James AR, Schroeder MP, Ortiz-Tanchez J, et al. Molecular alterations in bone marrow mesenchymal stromal cells derived from acute myeloid leukemia patients. *Leukemia* 2017;**31**:1069−78.
31. Corradi G, Baldazzi C, Očadlíková D, Marconi G, Parisi S, Testoni N, et al. Mesenchymal stromal cells from myelodysplastic and acute myeloid leukemia patients display *in vitro* reduced proliferative potential and similar capacity to support leukemia cell survival. *Stem Cell Res Ther* 2018;**9**:271.
32. Azadniv M, Myers JR, McMurray HR, Guo N, Rock P, Coppage ML, et al. Bone marrow mesenchymal stromal cells from acute myelogenous leukemia patients demonstrate adipogenic differentiation propensity with implications for leukemia cell support. *Leukemia* 2020;**34**:391−403.
33. Levis M. Arsenic and all-*trans* retinoic acid for acute promyelocytic leukemia: yes, it really is as good as it seems. *Haematologica* 2021;**106**:3031−2.
34. Gowen A, Shahjin F, Chand S, Odegaard KE, Yelamanchili SV. Mesenchymal stem cell-derived extracellular vesicles: challenges in clinical applications. *Front Cell Dev Biol* 2020;**8**:149.
35. Zhou Y, Zhou W, Chen X, Wang Q, Li C, Chen Q, et al. Bone marrow mesenchymal stem cells-derived exosomes for penetrating and targeted chemotherapy of pancreatic cancer. *Acta Pharm Sin B* 2020;**10**:1563−75.
36. Eirin A, Zhu XY, Puranik AS, Tang H, McGurren KA, van Wijnen AJ, et al. Mesenchymal stem cell-derived extracellular vesicles attenuate kidney inflammation. *Kidney Int* 2017;**92**:114−24.
37. Keshtkar S, Azarpira N, Ghahremani MH. Mesenchymal stem cell-derived extracellular vesicles: novel frontiers in regenerative medicine. *Stem Cell Res Ther* 2018;**9**:63.
38. Yeo RWY, Lai RC, Zhang B, Tan SS, Yin Y, Teh BJ, et al. Mesenchymal stem cell: an efficient mass producer of exosomes for drug delivery. *Adv Drug Deliv Rev* 2013;**65**:336−41.
39. Li JK, Yang C, Su Y, Luo JC, Luo MH, Huang DL, et al. Mesenchymal stem cell-derived extracellular vesicles: a potential therapeutic strategy for acute kidney injury. *Front Immunol* 2021;**12**:684496.
40. Zhao AG, Shah K, Cromer B, Sumer H. Mesenchymal stem cell-derived extracellular vesicles and their therapeutic potential. *Stem Cell Int* 2020;**2020**:8825771.

41. Cui C, Chakraborty K, Tang XA, Zhou G, Schoenfelt KQ, Becker KM, et al. Neutrophil elastase selectively kills cancer cells and attenuates tumorigenesis. *Cell* 2021;**184**:3163−3177.e21.
42. Ziv E, Koren R, Zahalka MA, Ravid A. TNF-alpha increases the expression and activity of vitamin D receptor in keratinocytes: role of c-Jun N-terminal kinase. *Dermatoendocrinol* 2016;**8**:e1137399.
43. Fabri M, Stenger S, Shin DM, Yuk JM, Liu PT, Realegeno S, et al. Vitamin D is required for IFN-gamma-mediated antimicrobial activity of human macrophages. *Sci Transl Med* 2011;**3**:104ra2.
44. Chen K, Aenlle KK, Curtis KM, Roos BA, Howard GA. Hepatocyte growth factor (HGF) and 1,25-dihydroxyvitamin D together stimulate human bone marrow-derived stem cells toward the osteogenic phenotype by HGF-induced up-regulation of VDR. *Bone* 2012;**51**: 69−77.
45. Gupta K, Stefan T, Ignatz-Hoover J, Moreton S, Parizher G, Saunthararajah Y, et al. GSK-3 inhibition sensitizes acute myeloid leukemia cells to 1,25D-mediated differentiation. *Cancer Res* 2016; **76**:2743−53.
46. Takeda Y, Harada Y, Yoshikawa T, Dai P. Chemical compound-based direct reprogramming for future clinical applications. *Biosci Rep* 2018;**38**:BSR20171650.
47. Xie X, Fu Y, Liu J. Chemical reprogramming and transdifferentiation. *Curr Opin Genet Dev* 2017;**46**:104−13.
48. Hou P, Li Y, Zhang X, Liu C, Guan J, Li H, et al. Pluripotent stem cells induced from mouse somatic cells by small-molecule compounds. *Science* 2013;**341**:651−4.
49. Johnson K, Zhu S, Tremblay MS, Payette JN, Wang J, Bouchez LC, et al. A stem cell-based approach to cartilage repair. *Science* 2012; **336**:717−21.
50. Wu X, Hu W, Lu L, Zhao Y, Zhou Y, Xiao Z, et al. Repurposing vitamin D for treatment of human malignancies *via* targeting tumor microenvironment. *Acta Pharm Sin B* 2019;**9**:203−19.
51. Deeb KK, Trump DL, Johnson CS. Vitamin D signalling pathways in cancer: potential for anticancer therapeutics. *Nat Rev Cancer* 2007;**7**: 684−700.
52. Boehm MF, Fitzgerald P, Zou A, Elgort MG, Bischoff ED, Mere L, et al. Novel nonsecosteroidal vitamin D mimics exert VDR-modulating activities with less calcium mobilization than 1,25-dihydroxyvitamin D3. *Chem Biol* 1999;**6**:265−75.
53. Swann SL, Bergh J, Farach-Carson MC, Ocasio CA, Koh JT. Structure-based design of selective agonists for a rickets-associated mutant of the vitamin D receptor. *J Am Chem Soc* 2002;**124**:13795−805.